


Nonlocal self-organization of a dissipative systemJaime Clark ^{1,2,*}, Felipe Torres,^{1,3} Laura Morales ^{4,5} and Juan Alejandro Valdivia ^{1,3}¹*Departamento de Física, Facultad de Ciencias, Universidad de Chile, Santiago 7800003, Chile*²*Facultad de Ciencias, Escuela de Ingeniería Civil Industrial, Universidad Mayor, Santiago 9170124, Chile*³*Centro para el Desarrollo de la Nanociencia y Nanotecnología (CEDENNA), Santiago 7500000, Chile*⁴*Universidad de Buenos Aires, Facultad de Ciencias Exactas y Naturales, Departamento de Física, Buenos Aires C1428EHA, Argentina*⁵*Universidad de Buenos Aires, Consejo Nacional de Investigaciones Científicas y Técnicas, Instituto de Física del Plasma (INFIP), Buenos Aires C1428EHA, Argentina* (Received 28 October 2020; revised 7 February 2021; accepted 16 February 2021; published 18 March 2021)

We study the self-organization process induced by a nonlocal critical field, in analogy with the electric field that is derived from the global spatial profile of electric charge density during a discharge. In this nontrivial extension of standard sandpilelike models of intermittent dissipation, the charges move in a similar manner to grains of sand when the threshold condition on the field is achieved. Here we focus our attention on the long term statistics of events, so that we consider an extremely simplified model in close similarity with sandpiles, avoiding some of the extremely interesting complexities that occur in three-dimensional electric discharges. For the observed avalanches (discharges in this case) we analyze four characteristic quantities: current, charge discharged, energy discharged, and duration of the discharge. We have run several simulations to explore the parameter space and found in general that they exhibit well defined power law event statistics spanning for one to three decades in general. For some parameter values we observe the existence of large or global events, in addition to the power law statistics, some of which may be related to finite size effects due to the size of the simulation box. This is the first step in understanding the long term statistics of systems with avalanches or discharges, when the criticality is controlled by nonlocality, as there are a number systems, such as lightning discharges or heat transport in tokamaks, where this type of dynamics is expected to occur.

DOI: [10.1103/PhysRevE.103.032127](https://doi.org/10.1103/PhysRevE.103.032127)**I. INTRODUCTION**

Self-organization (SO) plays a critical role in many types of driven out-of-equilibrium systems [1–12], particularly since the concept of self-organized criticality (SOC) was proposed by Bak, Tang, and Wiesenfeld [13]. It refers to driven systems with many degrees of freedom that can reach a global coherent state with intermittent dissipation events that follow self-similar event statistics [1,2,14]. One of the most popular models of SO is the sandpile model of Bak *et al.* [13], in which a local conservative dissipation event is produced when a local quantity, usually some type of slope or gradient, crosses a threshold. In this model, the hysteretic behavior plays a key role in the dissipation dynamics. The instantaneous state depends on the previous temporal evolution of the system enabling a loading phase different from the unloading one [15]. Therefore, the temporal evolution of the system describes a closed hysteresis loop where energy can be accumulated and, subsequently, released. This loop appears, as the local gradient becomes much lower than the one at the threshold condition after the local dissipation event, so that some loading (external or from its neighbors) must occur before a local dissipation can occur again. In the standard sandpile models the driver

needs to be injecting energy very slowly, but these restrictions can be lifted in some generalized versions of it [4,5,16,17].

These systems seem to evolve spontaneously to such a critical state due to their internal dynamics without tuning of an external parameter, except for a local threshold condition that triggers a local hysteretic and irreversible dissipation event. The universal behavior is usually somewhat independent of the particular local threshold condition and the event distributions are invariant in scale, so that they do not have spatial and/or temporal characteristic scales except for the finite system size. At first sight, it may resemble what happens in equilibrium systems close to a critical point where the only characteristic scale of the system is the correlation length which diverges at the critical temperature. However, the collective dissipation events are spatially inhomogeneous, as they occur in regions that display fractal boundaries for discharges in two or more dimensions [18–20]. This means that the system exhibits collective patterns with self-similarity and invariance in the spatial scales as well.

As mentioned above, the critical behavior found in these sandpile-type models is produced by a local threshold or critical condition, such that a local scalar quantity gets partially transported to the neighbors (usually in discrete quantities) in a local hysteretic dissipation event when a local gradient of the same scalar quantity reaches a threshold at a particular cell. Of course, as a certain amount of the conserved scalar quantity is transferred to the neighbors, they can then become unstable

*jclark@ug.uchile.cl

and dissipate by the same dynamics. Hence, the dynamical interaction of local dissipations can produce large collective dissipation events of all sizes, with no particular spatial or temporal correlation scales, except for that determined by the finite size of the system.

In this paper, we study a similar intermittent loading-unloading behavior but with nonlocal dissipation dynamics, which will be implemented with an additional spatially dependent quantity that is computed from the nonlocal properties of the original scalar quantity. One analogy of this situation is electric discharges in which charges, the scalar quantity that is conserved, move when a threshold condition for the electric field, a nonlocal quantity that is computed from the scalar quantity, crosses a threshold. Similar nonlocal behavior also seems to be occurring in magnetic reconnection [5,6] and turbulent heat transport in tokamaks [16]. In the next section we describe in detail how such dynamics could be implemented through a highly simplified, but robust, model that includes some of the main ingredients discussed above. For the rest of the section, we will continue analyzing the analogy with electric discharges, in particular lightning discharges that occur during thunderstorms, and sometimes during volcanic eruptions or dust storms [21–24]. We compare the electric discharge inspired and sandpile type of models that will provide the intuition for the construction of our highly simplified model in the next section.

Lightning discharges are an interesting phenomenon that have a lot of relevance for the chemistry of the tropospheric dynamics and climate, in determining the global atmospheric electric field, among others [25–27]. There are different types of lightning discharges such as cloud to cloud (CC), ground to cloud (GC), cloud to ground (CG), etc. In particular, CG lightning discharges are the second most common followed by intracloud lightning. There are some 2.5×10^7 cloud to ground lightning strokes over the world every year, and its number is expected to continue to increase due to global warming [28]. The CG lightning discharges can be further separated into positive lightning discharges and negative lightning discharges, the latter being responsible for 90% of the activity in CG discharges [29]. Currently, there is a lot of research conducted to understand the details and complexities of how discharges are produced and its subsequent dynamics. In general, we can mention that positive and negative charges get separated inside the clouds, probably by the wind induced dynamics of ice [25], which would correspond to the driver in the sandpile language. Understanding the lightning discharge event statistics, and what controls it, can become a research endeavor with profound consequences for our future climate [30] and for our immediate well being as may be reflected in the recent increase in large forest fires in the U.S.A. [31,32] and many other countries such as Chile. For example, in August 2020 we saw an extremely large dry thunderstorm called the August lightning siege in California (U.S.A.) that ignited around 650 wildfires due to a set of large and strong lightning events combined with low humidity and a relative high temperature that facilitates the fire ignition and burning of dry vegetation [33,34].

Similarly, there is a lot of interest on the complex processes that are involved on lightning initiation, that may include electric breakdown that seems to be consistent with initial

breakdown electromagnetic pulses and/or runaway electrons that seem to explain observations of x rays and positron emissions [35–39]. Since we are trying to understand the long term statistics of nonlocally induced discharges, and to stay as close as possible to sandpile-type models, we may consider for simplicity and illustration purposes that charges move during a discharge when the local value of the electric field goes over a fixed threshold value. Of course, electric charge motion in lightning discharges includes complex processes of charge ionization, electric field intensification, attachment, etc. That requires high performance computing simulations [40] making difficult the construction of large event statistics. The lightning models based on regular or runaway breakdown require a threshold field that depends on the local pressure. Additionally, there are some indications that dust particles may also influence the threshold field [41]. Here we will assume that the electric field threshold value will be fixed in time and uniform for the whole simulation box, and leave more sophisticated variants for future papers.

Lightning discharges do produce self-similar power law event distributions for current, charge discharged, energy dissipation, etc. [29], resembling the equivalent self-similar event distributions of sandpilelike models. Furthermore, it is possible to observe that the global dissipation events of lightning discharges also occur over a fractal characterized with the zigzag type process of the stepped leader [42]. The current flows through the dielectric media in a similar way as in Ohm's law, where the charge displays an active one-dimensional motion along the voltage gradient. There have been a number of proposed models that have attempted to reproduce qualitatively these fractal structures that are observed in photographs and up into the ionosphere [27,43–47], however, these models were more concerned with describing the self-similar spatial structure of a particular discharge or the self-similar long term event statistics of a large number of discharge events.

II. MODEL

We will present a generalization of a sandpile-type model that has dissipation events induced by a nonlocal threshold condition, in analogy with negative CG cloud discharges. Hence, one important point is that in the standard sandpile type (not ours) of models the threshold condition is computed from the local information, while in our situation the threshold condition is over the nonlocal electric field, that in this paper will depend only on the global spatial profile of the charge density.

As mentioned above, in sandpile-type model the critical behavior is quite insensitive to the particular details of the dissipation, except that it occurs when a local gradient of the scalar quantity is exceeded. Here, we will not concentrate on the particular complexities of the lightning initiation and discharge evolution details, but instead we will consider a highly simplified version of the discharges, to stay as close as possible to sandpilelike models. The idea is to study the long term self-similar distribution of dissipation events by being able to run the simulation over a very long time.

Hence, we will consider a one-dimensional (1D) current flow in a box with L discrete cells in which the spatial density

profile $\rho(x, t)$ of the negative charge evolves, maintaining the essential complexity of the nonlocal self-organized behavior of a dissipative system. Note that the branching process, usually a two-dimensional phenomenon, that is capable of producing dissipation events over a fractal will be analyzed in a future paper. The out-of-equilibrium system will be driven, as for sandpile-type models, by dropping a discrete amount of charge at some randomly chosen cell sites of the domain box trying to simulate the charge separation dynamics that occurs inside the clouds. The inhomogeneous time dependent spatial density profile $\rho(\mathbf{r}, t)$ produces a time dependent field $E(\mathbf{r}, t)$ that is computed from

$$E(\mathbf{r}, t) = -\nabla\Psi(\mathbf{r}, t),$$

where the scalar potential $\Psi(\mathbf{r}, t)$ satisfies

$$\nabla^2\Psi(\mathbf{r}, t) = -4\pi\rho(\mathbf{r}, t).$$

Therefore, the scalar potential can then be computed from a suitable Green's function as

$$\Psi(\mathbf{r}, t) = \int_V G(\mathbf{r}, \bar{\mathbf{r}})\rho(\bar{\mathbf{r}}, t)d\bar{V}.$$

For simplicity in this 1D geometry we take the Green's function as

$$G(x, \bar{x}) = \frac{1}{\sqrt{|x - \bar{x}|}} - \frac{1}{\sqrt{|x + \bar{x}|}},$$

which is consistent with a grounded conducting lower boundary condition $G(x = 0) = 0$. A one-dimensional dielectric lattice of length L is considered, so that sites are numbered as $x = i = 1, \dots, L$. We define the discretized variables $\rho(x = i, t) = \rho_i(t)$, $\Psi(x = i, t) = \Psi_i(t)$, and $E(x = i, t) = E_i(t)$ at the grid points of the lattice. Technically speaking, so that the units can be translated, ρ_i represents the charge contained in the i th cell. The potential and electric fields are computed from the Green's function for a given density profile ($i > 0$) as

$$\Psi_i(t) = \sum_{j \neq i}^L \rho_j(t)G(i, j) \quad (1)$$

and

$$E_i(t) = -\sum_{j \neq i}^L \rho_j(t)G_x(i, j), \quad (2)$$

where $G_x(x, \bar{x})$ is the partial derivative of $G(x, \bar{x})$ with respect to x . We assume that the ground is able to immediately dispose of any charge that reaches $x = 0$ ($i = 0$) so that $\rho_0(t) = 0$. The inlet is the region close to $i = L$ and the outlet region is at $i = 0$. Here, we run the simulations with $L = 60$ cells, leaving a quantitative analysis of finite size effects for a future work. Hence, the charges that reach the outlet at $i = 0$ are discharged (taken out of the system) instantaneously to guarantee the grounded condition there. We define Q_G as the sum of all the charges that reach the ground at $i = 0$ during the discharge. Let us note that this Green's function is scale invariant, so in essence our 1D model results become universal.

Unit amounts of charge will be dropped randomly in space but close to the top of the simulation box, namely, at $x > 0.8L$. Due to the boundary condition we can think that there are

image charges below the ground, so that the charges in the simulation will have a tendency to move towards the ground attracted by these image charges. Let us note that in this sense, the electric field is a nonlocal quantity that depends on the global spatial density profile.

Again, our very simplified model of nonlocal dissipation does not consider all the very complex and interesting phenomenology of lightning discharges. Instead, our highly simplified model is expected to contain some of the robust physical processes present in sandpilelike models, but with the nonlocal dissipation threshold that is natural in electrical discharges. Hence, in analogy with negative CG discharges, in this simplified model we will move a percentage of the charge present at the particular cell of the simulation box in the direction of the local electric field if it is larger than some threshold value, namely, $E_i > E_c$. In the electric discharge analogy E_c would be related to the threshold electric field value of the dielectric medium in which the rupture is generated. Hence, depending on the value of the electric field at a site, the site may be active or passive. More precisely, if $E_i(t) > E_c$ then some amount of charge at that site i is transferred to its left neighbor ($i - 1$) so that the conservative charge dynamics are

$$\begin{aligned} \rho_i(t + 1) &= \rho_i(t) - \kappa\rho_i(t), \\ \rho_{i-1}(t + 1) &= \rho_{i-1}(t) + \kappa\rho_i(t), \end{aligned} \quad (3)$$

where κ denotes the percentage of $\rho_i(t)$ that is moved towards the next cell at $i - 1$. Other possibilities could involve moving a fixed amount of charge to the next cell, but we will leave the case of these variants for a future paper. The simulation dynamics goes as follows. There are three "counters" in the system, one is the time n that accounts for the "discharge" time step. This time step n is divided into a number of iterations j ($j = 1, \dots, \tau_n$) so that we have different spatial profiles of the potential, electric field, and density at each $n : j$ instance of the τ_n iterations within a discharge n . Finally, t is a global iteration counter that counts the number of iterations from beginning of the simulation, namely, $t = \sum_{m=1}^{n-1} \tau_m + j$. The n th discharge starts with the first iteration $j = 1$ during the loading of a unit of charge at a random position close to the top of the simulation box, requiring a recalculation of $\Psi_i(t)$ and $E_i(t)$. If none of the cells that have charge become unstable [$E_i(t) < E_c$], then we say that the discharge n had only $\tau_n = 1$ iterations. If some of the cells become unstable [$E_i(t) > E_c$], then in each iteration we simultaneously move the charge in all the unstable sites where $E_i(t) > E_c$. At each iteration we have to recalculate the potential and electric field since the density spatial profile has changed. We repeat this process τ_n times until all of the cells that have charge satisfy $E_i(t) < E_c$. A global discharge event considers a duration of multiple τ_n iterations that produce a large number N_D of local dissipations, from the moment a charge is dropped into the system until the local dissipations it produces stops.

In the process we can compute the total current I , or charge that moved, during the discharge event. We can also compute the energy dissipated during the discharge event, where the energy at any time during the simulation is given by

$$\epsilon(t) = \frac{1}{2} \int \Psi(x, t)\rho(x, t)dx \rightarrow \frac{1}{2} \sum_{i=0}^L \Psi_i(t)\rho_i(t), \quad (4)$$

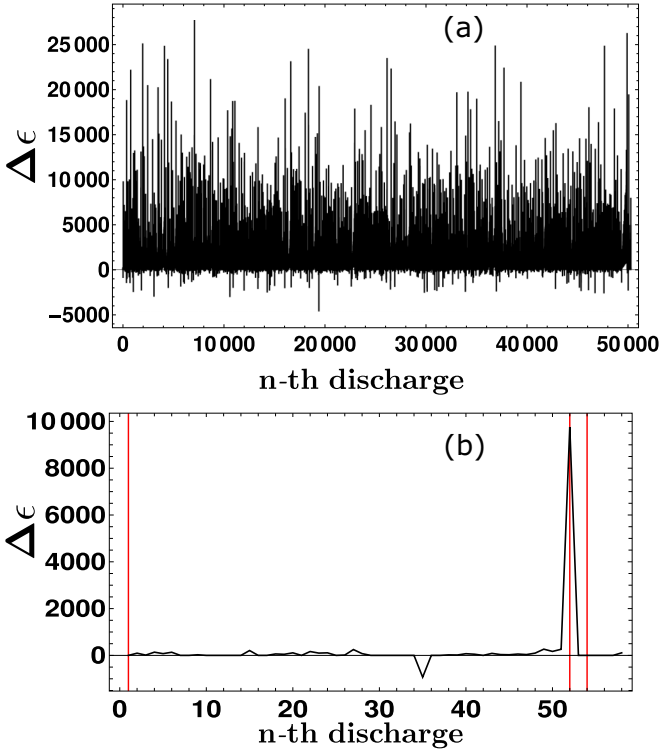


FIG. 1. (a) Energy dissipated $\Delta\epsilon$, as the difference in energy (4) between the final (when discharge stops) and initial (right after the driving charge is dropped into simulation) density profiles, for each discharge during 50 000 driving cycles for $L = 60$, $E_c = 4$, $\kappa = 0.5$. (b) A zoom of the energy dissipated for the first 54 discharge events in the simulation.

in analogy with electric discharges. The system evolves with these simple rules that resemble a sandpile-like behavior, but with a nonlocal threshold condition that depends on the nonlocal electric field. In Fig. 1(a) we observe the energy dissipated during each discharge event for a particular simulation. The energy dissipated during the discharge

$$\Delta\epsilon_n = \epsilon(t_{n:\tau_n}) - \epsilon(t_{n:1}) \quad (5)$$

is then the energy difference between the profiles at $n : \tau_t$ and $n : 1$, the latter right after the added charge is dropped into the simulation at the n th driving cycle. Hence, each peak is associated with each drop of charge into the system and subsequent release of energy during the n th global discharge event. We note in Fig. 1(b) that sometimes there is no dissipation when a charge is dropped into the system, so that the system can go into a process of loading that eventually leads to a relatively large unloading event. This is the basis for the generation of self-similar power law statistics, in which the hysteresis plays a fundamental role.

To observe and corroborate that the discharges or avalanches are being generated, the profiles of the charge density, potential, and electric field are shown in Fig. 2 for the $n = 1$, 52, and 54 discharges corresponding to each of the three discharge events marked at the three vertical lines of Fig. 1(b). We note from Fig. 2(a) at $n = 1$ that the system is slowly charging as charge is deposited at the top of the simulation box. For a while, only a small amount of charge moves trying

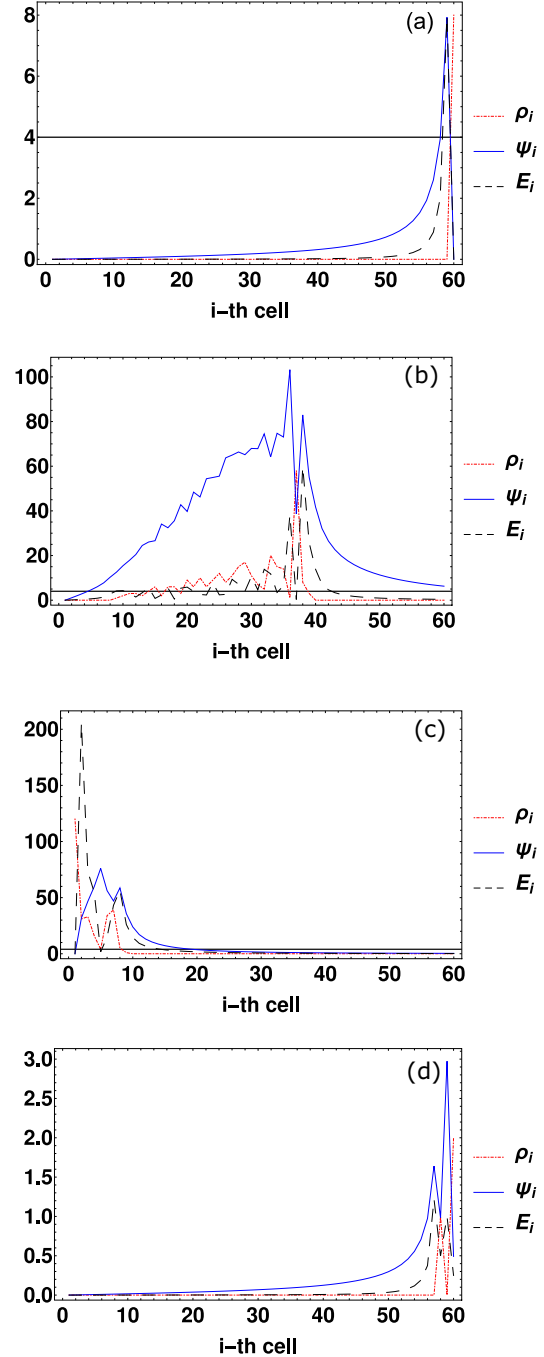


FIG. 2. Spatial variation of the charge density (dot-dash red curve), potential (continuous blue curve), and electric field (dashed black curve) at (a) the beginning of the $n = 1$ discharge (iteration 1 : 1), (b) the beginning of the $n = 52$ discharge (iteration 52 : 1), (c) the middle of the $n = 52$ discharge (iteration 52 : 187), and (d) the end of the $n = 54$ discharge (iteration 54 : 1) corresponding to the vertical lines in Fig. 1(b). It can be clearly distinguished how a global avalanche is generated in which the system transports, in an intermittent fashion, a large amount of charge to the ground where it is eliminated. The units of the quantities are in simulation units. It is important to notice that we are not considering ionization, therefore, it can be seen from (a) that there is an electric field greater than the threshold, but there is no charge at that cell to move at that particular time. The $n = 52$ discharge took 187 iterations, for $E_c = 4$, $\kappa = 0.5$, and $L = 60$. The black horizontal line corresponds to E_c .

to locally dissipate the field produced by the dropped charges until we reach $n = 52$ of Fig. 2(b). Here, we observe a large amount of charge that has accumulated and that could move towards the ground $i = 0$. A few iterations later, during the same $n = 52$ global discharge event, we observe in Fig. 2(c) that a large percentage of the accumulated charge is moving to the ground where it leaves the system. Once the discharge event finishes, we see in Fig. 2(d) a spatial profile at the end of the $n = 54$ discharge that is similar, although not equal, to the one before the large discharge event occurs, namely at $n = 1$.

Hence, in analogy with the lightning discharges, we note from Fig. 2 that the system begins to accumulate charge at the cloud top in analogy to the charge separation and storm's electrification processes [48]. The analogous charge separation is simulated as the charge that is being dropped at the top part of the simulation box once a discharge event is finished. This increases the energy of the system. These loading events eventually produce an accumulation of charge so there will be areas where the electric field will exceed the critical threshold E_c , which will allow the charge to move through the system in the direction of the ground until the system relaxes completely. Usually, we see small discharge events, however, there are times at which the system discharges a large amount of charge to the ground.

In Fig. 3 we show the distributions of charge duration τ [Fig. 3(a)], total charge discharged at the ground Q_G [Fig. 3(b)], and energy dissipated $\Delta\epsilon$ [Fig. 3(c)] for a large set of events. We note that for these parameter values, the distribution of τ , Q_G , and $\Delta\epsilon$ seems to display power law distributions in a certain range of values, in combination with large "more global" events. Intuitively, we expect that these large global events would be affected by the finite size of the simulation box for they correspond to the situation displayed for the $n = 52$ discharge in Fig. 2 where a relatively large amount of charge is removed from the system. This is quite different from what is observed in regular sandpile-type models for the long term event statistics. We now analyze how the relative importance of these two regimes, and particularly the validity of the power law event distributions, depends on the critical electric field E_c and percentage κ of charge that moves when the local electric field becomes greater than E_c . The index of the power law distributions is constructed by a maximum likelihood estimator. In Fig. 4 we study how the distributions of energy dissipation change as we vary these two parameters.

To study the range of validity of these power law event distributions, we change the two main free parameters that govern the dynamics, which are the critical electric field E_c and the percentage κ of charge that moves when the local electric field becomes greater than E_c . In Fig. 4 we study how the distributions of energy dissipation change as we vary these two parameters. We note from Fig. 4(a) that for a low critical value of the electric field the system does not offer resistance for the movement of charge and, therefore, for the generation of discharges. While, for a high value of E_c the system should generate few discharges where a greater amount of accumulated energy in the system is dissipated.

Similarly, we note from Fig. 4(b) that if one varies the percentage of charge that moves when the local electric field becomes larger than E_c , having a low value, will allow a

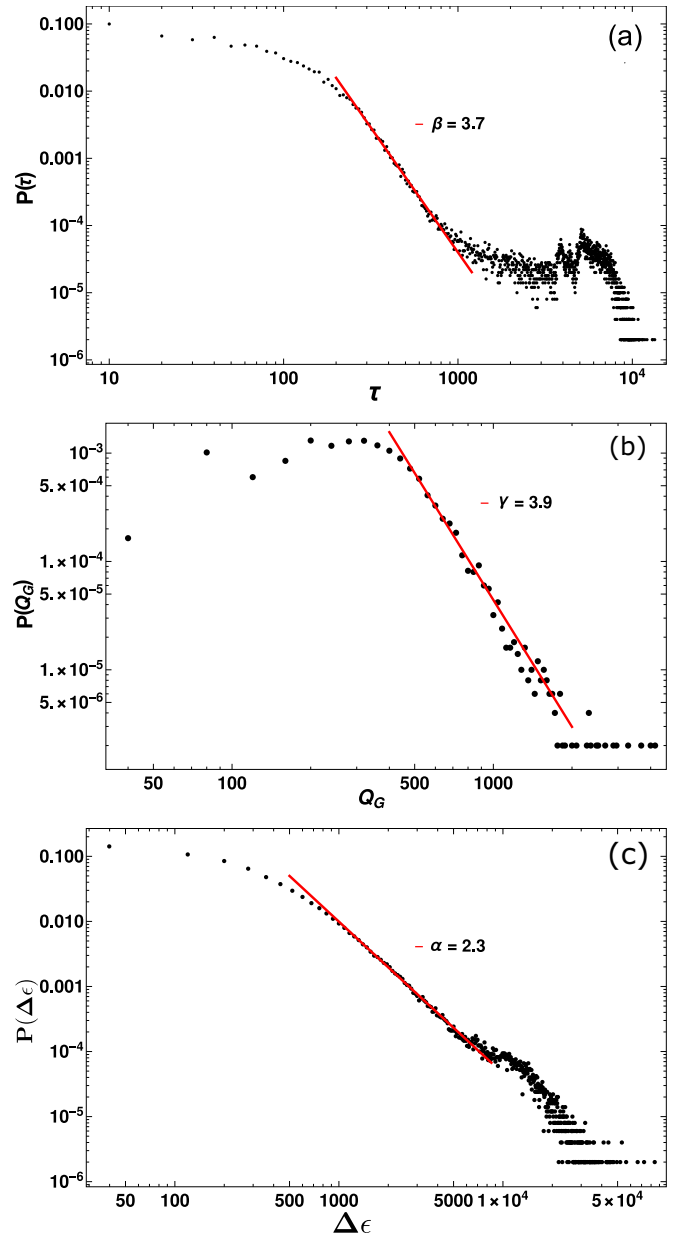


FIG. 3. Probability density for the (a) duration τ , (b) total charge Q_G lost at the ground, and (c) energy dissipated $\Delta\epsilon$ during the global discharges, respectively. The parameters are the same as in Fig. 2. We use $L = 60$, $\kappa = 0.5$, and $E_c = 4.0$.

greater accumulation of charge and a lower number of electric discharges but of larger energy dissipated. If the percentage is high, there will be a large amount of movement of charges and it will become very easy for the system to generate electric discharges but of smaller amounts of energy dissipated. We clearly see that at very high critical electric field values the system tends to accumulate a lot of charge and, therefore, the variations of dissipated energy increase. Similarly, for a low percentage of charge movement, the system exhibits a similar trend, where large amounts of dissipated energy are found. For the other case, we observe self-similar statistics.

We can do the same for the current I , namely, the amount of charge that is moving in the system during a discharge.

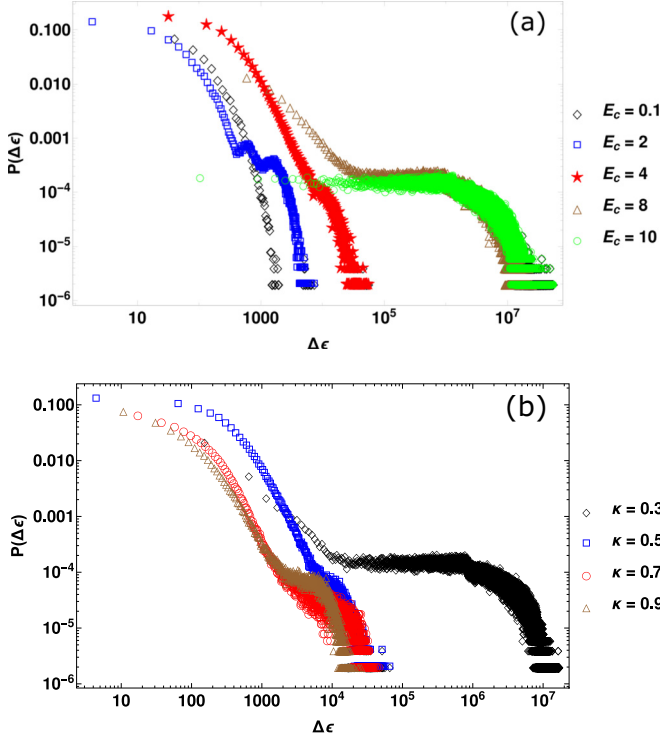


FIG. 4. (a) Probability density for energy dissipated $\Delta\epsilon$ for different values of E_c . We use $\kappa = 0, 5$. (b) Probability density for the current produced by different values of κ . We use $E_c = 4$. Simulations are done for $L = 60$ cells.

The distributions of current are shown in Fig. 5 as we vary E_c [Fig. 5(a)] and κ [Fig. 5(b)]. Interestingly enough we see events with self-similar statistics for relatively low values of E_c and large values of κ .

In general, we note the distribution of events for the discharges, namely, the energy discharged, the duration, the charge discharged at the ground, and the current during the discharge; display power law statistics over a finite range of values. For example, in the case of the energy discharged we expect a power law behavior given by

$$P(\Delta\epsilon) \sim \Delta\epsilon^{-\alpha},$$

where α is the power law index. We note that α varies with E_c and κ as suggested by Fig. 3. In Fig. 6(a) we display this variation with E_c for fixed value of $\kappa = 0.5$. The other measures of the discharges have similar power law behavior. There is an interesting interplay of self-similar and large (global) dissipation events, particularly for large values of E_c where the system size must also play a role. The variation of this critical behavior with the system size will be analyzed in a future paper.

In order to understand the relevance of the power law behavior found in this paper for nonlocal critical dissipation, we will compare with a sandpile-type model with local critical dissipation. There are a number of variants of the classic sandpile proposed by Bak [13], by considering different types of evolution dynamics, threshold conditions, type and value of hysteresis, boundary conditions, etc., that at the end produce different types of distribution of events (i.e., power law

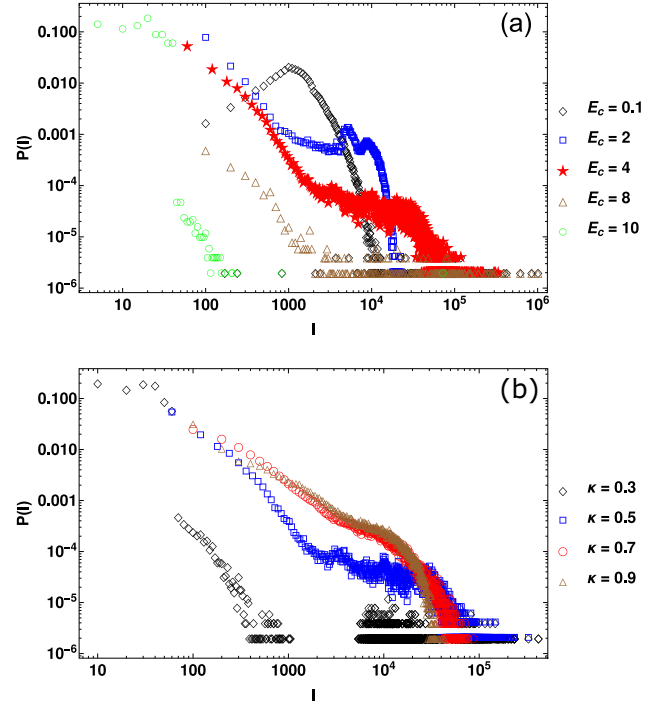


FIG. 5. (a) Probability density for the current produced by different critical electric fields E_c . We use $\kappa = 0, 5$. (b) Probability density for the current produced by different values of κ . The value of $E_c = 4$. Simulations are done for $L = 60$ cells.

index in the case of power law distributions) such as energy dissipation [11,49–52]. The type and value of the hysteresis, which in some models may be difficult to relate directly to the dissipation, can affect considerably the allowed range of sizes of these dissipation events. For comparison, we will estimate the variation of the critical exponent α for the dissipated energy. We consider a 1D sandpile model, but with a variation respect to the original Bak [13] case, so that the results are more readily comparable with our nonlocal discharges. Particularly, we used open boundary conditions for both ends of the cellular automaton, as

$$h_0 = 0,$$

$$h_L = 0.$$

Hence, the boundaries are open in the sense that any grain that reaches the boundaries is taken out of the system, in the same spirit as in our nonlocal discharges. The length of the box for this simulation is $N = 100$ cells and we apply the dissipation rule to each cell as

$$h_i(t+1) = h_i(t) - 2,$$

$$h_{(i\pm 1)}(t+1) = h_{(i\pm 1)}(t) + 1$$

when $\nabla^2 h(x) \rightarrow h_i - (h_{(i+1)} + h_{(i-1)})/2 > Z_c$. Here h_i represents the number of grains present at cell i and Z_c is the critical value that activates the dynamics. Note that this type of sandpile model, where the toppling condition depends on a critical value of local Laplacian, has been studied by [53], and it is also similar to the ones used for magnetic dissipation in the solar context [52]. The energy can be calculated from an

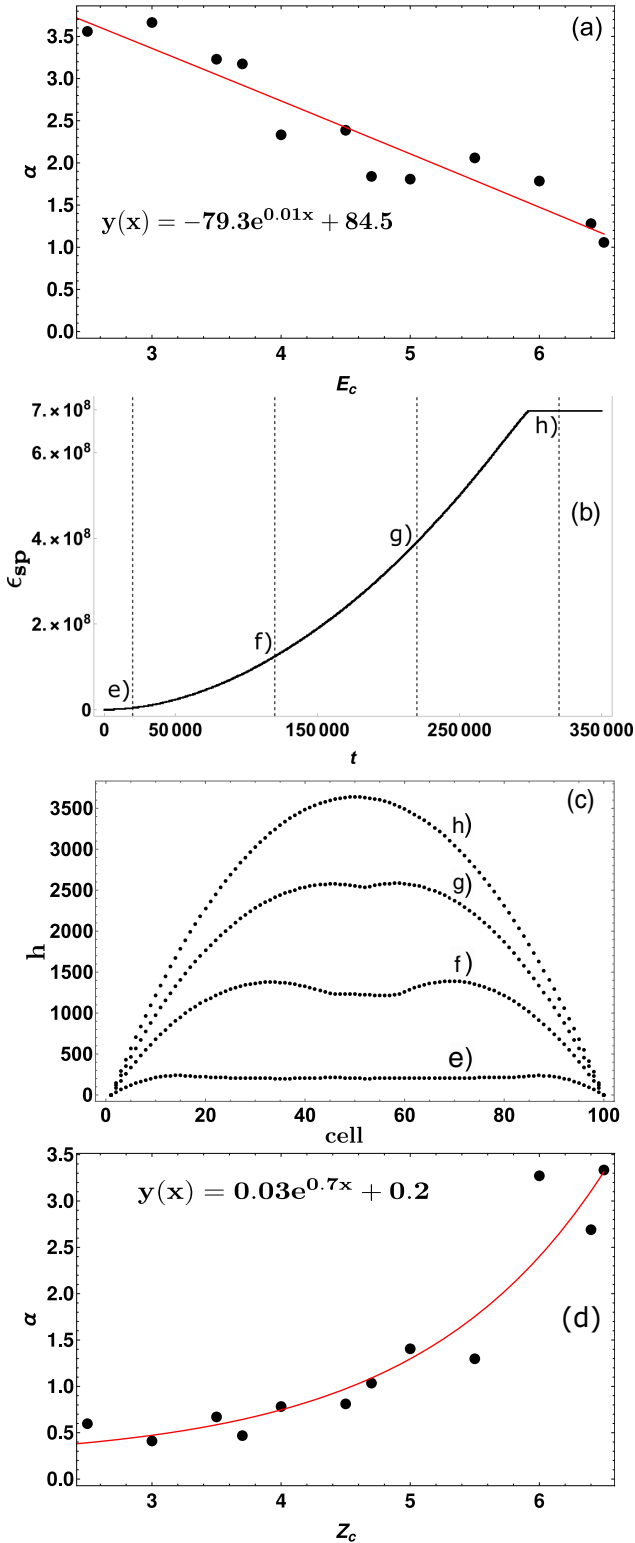


FIG. 6. (a) Variation of the critical exponent α as a function of the threshold value E_c . We used $\kappa = 0.5$. (b) Energy as a function of time for the variant of the standard sandpile with $N = 100$ and $Z_c = 4$. (c) Different spatial profiles as we approach the critical asymptotic state at the times marked as vertical lines in (b). (d) For comparison, we show the variation of α for the variant of the standard sandpile by Bak *et al.* [13] as a function of Z_c , an equivalent critical local slope.

equivalent formula, namely,

$$\epsilon_{sp} = \int \rho \Psi dx \approx A \int h(x)^2 dx \rightarrow \epsilon_{sp}(t) = \sum_{i=1}^N h_i^2(t)$$

since the potential Ψ is now the external local gravitational potential. Here A is a constant that we set to 1. In Fig. 6(b), we show the time series of the lattice energy for the variant of the standard sandpile as a function of time, showing that it reaches an asymptotic critical dynamical state (with hysteresis) at around $t = 3 \times 10^5$. Similarly, in Fig. 6(c) we display the intermediate states at the times marked with a vertical line in Fig. 6(b) to display how the asymptotic state is approached in the spatial domain. This points to the growth of the midfield as the system approaches the critical state, similar to the idea developed in [54]

It is interesting to note that, despite the fact that this is a variation of the standard sandpile in one dimension, it does produce self-similar event statistics for a range of parameters. We display in Fig. 6(d) the value of α as a function of Z_c for the power law event distribution of energy dissipated in the above variation of the sandpile that considers only local dissipation. We note an interesting variation of α with Z_c , but is quite different from the variation of the distribution of energy dissipation produced by the nonlocal discharges with E_c . In fact, the power law index in these systems [comparing Figs. 6(a) and 6(d)] has the opposite trend with respect to the critical threshold value, demonstrating that there is a significant difference in the universality class of the local and nonlocal dissipation models, apart from the fact that in the case of the model with nonlocal dissipation the power law behavior coexists with global events. Intuitively, for our nonlocal discharge model we do expect the power law index for energy dissipation to decrease as we increase E_c because in essence we increment the probability of allowing larger events [Fig. 4(a)], i.e., smoothing out the distribution. Of course, the situation is not as simple as can be observed in the strange variation of the distribution of current in Fig. 5(a) as we increase E_c . We plan to use analytic approaches to study this system in future work.

III. SUMMARY

We presented a theoretical extension of sandpilelike models where the criticality is controlled by a nonlocal threshold condition, in analogy with electric discharges. The system was built in one dimension, for simplicity, that allows to generate discharges in one dimension. We analyze their long term event statistics and found power law distributions for some range of parameters, primarily the critical field E_c and percentage of charge discharged κ when the local electric field goes above this critical field. Of particular interest are the self-similar distributions of energy dissipated, duration, charge discharged, and current during the discharge. It is interesting to note that power law event distributions are also found in the analogous lightning discharges, however, the power law index may vary considerably due the inherent complexity and conditions that can affect such electric discharges. As expected, the power law event distribution gets broken for large critical fields or small κ , as large events, in which a relevant percentage of the

charges in the simulation box get discharged, appear in the system.

In the future we will extend the model to two and three dimensions to study how the power law event distributions change for the aforementioned parameters, and how the dissipation that is expected to occur in sets with fractal boundaries, as can be seen in sandpilelike models, appears in our model. We also plan to include ionization in the discharges, that is expected to change somehow the universal nature of the power law event statistics.

We hope that these types of analysis can improve our understanding of the long term statistics of a system that displays self-organization but where the criticality is controlled by a nonlocal threshold condition, as is expected to occur in a number of physical settings of interest where avalanches may

occur, such as electric discharges, magnetic reconnection, tokamak operation, etc.

ACKNOWLEDGMENTS

This work was funded by the National Agency for Research and Development (ANID)/Fondecyt under Award No. 1190703 (J.A.V.) and Conicyt doctoral Fellowship No. 21161595 (J.C.). We thank the support of CEDENNA. F. Torres acknowledges financial support from Grants No. FA9550-16-1-0122, No. FA9550-18-1-0438, Fondecyt 1160639, and CEDENNA through the Financiamiento Basal para Centros Científicos y Tecnológicos de Excelencia-FB0807. We acknowledge a number of discussions with Dr. P. Moya, Dr. V. Muñoz, and Dr. J. Rogan.

-
- [1] J. Hesse and T. Gross, *Front. Syst. Neurosci.* **8**, 166 (2014).
- [2] H. J. Jensen, *Self-organized Criticality: Emergent Complex Behavior in Physical and Biological Systems*, Vol. 10 (Cambridge University Press, Cambridge, 1998).
- [3] B. Carreras, D. Newman, V. Lynch, and P. Diamond, *Phys. Plasmas* **3**, 2903 (1996).
- [4] E. T. Lu, *Phys. Rev. Lett.* **74**, 2511 (1995).
- [5] A. J. Klimas, J. A. Valdivia, D. Vassiliadis, D. N. Baker, M. Hesse, and J. Takalo, *J. Geophys. Res.* **105**, 18765 (2000).
- [6] J. A. Valdivia, J. Rogan, V. Muñoz, B. A. Toledo, and M. Stepanova, *Adv. Space Res.* **51**, 1934 (2013).
- [7] B. Gutenberg and C. F. Richter, *Seismicity of The Earth and Associated Phenomena* (Princeton University Press Princeton, NJ, 1954).
- [8] K. Christensen and N. R. Moloney, *Complexity and Criticality* (Imperial College Press, London 2005).
- [9] D. Sornette, *Critical Phenomena in Natural Sciences: Chaos, Fractals, Selforganization, and Disorder: Concepts and Tools*, 2nd ed., Springer Series in Synergetics (Springer, Berlin, 2006).
- [10] M. J. Aschwanden, *Self-Organized Criticality in Astrophysics* (Springer, Berlin, 2011).
- [11] G. Pruessner, *Self-Organised Criticality* (Cambridge University Press, Cambridge, 2012).
- [12] C. Paul, *Natural Complexity: A Modeling Handbook* (Princeton University Press, Princeton, NJ, 2017).
- [13] P. Bak, C. Tang, and K. Wiesenfeld, *Phys. Rev. Lett.* **59**, 381 (1987).
- [14] G. Zipf, *The Psycho-Biology of Language* (Houghton Mifflin, Oxford, England, 1935).
- [15] J. A. Valdivia, J. Rogan, V. Munoz, and B. Toledo, *Space Sci. Rev.* **122**, 313 (2006).
- [16] V. Tangri, A. Das, P. Kaw, and R. Singh, *Phys. Rev. Lett.* **91**, 025001 (2003).
- [17] S. C. Chapman, N. W. Watkins, R. O. Dendy, P. Helander, and G. Rowlands, *Geophys. Res. Lett.* **25**, 2397 (1998).
- [18] C. Tebaldi, M. De Menech, and A. L. Stella, *Phys. Rev. Lett.* **83**, 3952 (1999).
- [19] B. B. Mandelbrot and J. A. Wheeler, *Am. J. Phys.* **51**, 286 (1983).
- [20] H. Hoffmann and D. Payton, *Sci. Rep.* **8**, 2358 (2018).
- [21] E. W. B. Gill, *Nature (London)* **162**, 568 (1948).
- [22] R. Anderson, S. Gathman, J. Hughes, S. Bjrnsso, S. Jnasson, D. C. Blanchard, C. B. Moore, H. J. Survilas, and B. Vonnegut, *Science* **148**, 1179 (1965).
- [23] A. K. Kamra, *Nature (London)* **240**, 143 (1972).
- [24] R. J. Thomas, P. R. Krehbiel, W. Rison, H. E. Edens, G. D. Aulich, W. P. Winn, S. R. McNutt, G. Tytgat, and E. Clark, *Science* **315**, 1097 (2007).
- [25] V. Rakov and M. Uman, *Lightning: Physics and Effects* (Cambridge University Press, Cambridge, 2003).
- [26] C. G. Price, *Surv. Geophys.* **34**, 755 (2013).
- [27] O. A. van der Velde, J. Montanyà, J. A. López, and S. A. Cummer, *Nat. Commun.* **10**, 4350 (2019).
- [28] D. M. Roms, J. T. Seeley, D. Vollaro, and J. Molinari, *Science* **346**, 851 (2014).
- [29] M. A. Uman and E. P. Krider, *IEEE Trans. Electromagn. Compat.* **EMC-24**, 79 (1982).
- [30] E. R. Williams, *Atmos. Res.* **76**, 272 (2005).
- [31] T. Brown, S. Leach, B. Wachter, and B. Gardunio, *Bull. Am. Meteorol. Soc.* **101**, S1 (2020).
- [32] K. J. Balch, B. A. Bradley, J. T. Abatzoglou, R. C. Nagy, E. J. Fusco, and A. L. Mahood, *Proc. Natl. Acad. Sci. U.S.A.* **114**, 2946 (2017).
- [33] US department of commerce and NOAA's national weather service. fire weather topics: Dry thunderstorms, <https://www.weather.gov/abq/clifeature2010drythunderstorms>.
- [34] August 2020 california lightning wildfires: the lightning siege, https://en.wikipedia.org/wiki/August_2020_California_lightning_wildfires.
- [35] S. Karunarathne, T. C. Marshall, M. Stolzenburg, N. Karunarathna, L. E. Vickers, T. A. Warner, and R. E. Orville, *J. Geophys. Res.: Atmospheres* **118**, 7129 (2013).
- [36] A. V. Gurevich, G. M. Milikh, and J. A. Valdivia, *Phys. Lett. A* **231**, 402 (1997).
- [37] A. Gurevich, Y. Medvedev, and K. Zybin, *Phys. Lett. A* **329**, 348 (2004).
- [38] T. Enoto, Y. Wada, Y. Furuta, K. Nakazawa, T. Yuasa, K. Okuda, K. Makishima, M. Sato, Y. Sato, T. Nakano *et al.*, *Nature (London)* **551**, 481 (2017).
- [39] G. Milikh and R. Roussel-Dupré, *J. Geophys. Res.* **115**, A00E60 (2010).

- [40] Y. P. Raizer, G. M. Milikh, and M. N. Shneider, *J. Geophys. Res.* **115**, A00E42 (2010).
- [41] T. Pähtz, H. Herrmann, and T. Shinbrot, *Nat. Phys.* **6**, 364 (2010).
- [42] C. J. Readings, *Q. J. R. Meteorol. Soc.* **112**, 562 (1986).
- [43] J. Sañudo, J. B. Gómez, F. Castaño, and A. F. Pacheco, *Nonlin. Process. Geophys.* **2**, 101 (1995).
- [44] L. Niemeyer, L. Pietronero, and H. J. Wiesmann, *Phys. Rev. Lett.* **52**, 1033 (1984).
- [45] J. A. Valdivia, G. Milikh, and K. Papadopoulos, *Geophys. Res. Lett.* **24**, 3169 (1997).
- [46] J. A. Valdivia, G. M. Milikh, and K. Papadopoulos, *Radio Sci.* **33**, 1655 (1998).
- [47] J. A. Riousset, V. P. Pasko, P. R. Krehbiel, R. J. Thomas, and W. Rison, *J. Geophys. Res.* **112**, D15203 (2007).
- [48] M. L. Gauthier, W. A. Petersen, L. D. Carey, and H. J. Christian Jr., *Geophys. Res. Lett.* **33**, L20803 (2006).
- [49] P. Ruelle and S. Sen, *J. Phys. A: Math. Gen.* **25**, L1257 (1992).
- [50] H. Flyvbjerg, K. Sneppen, and P. Bak, *Phys. Rev. Lett.* **71**, 4087 (1993).
- [51] K. Christensen, Á. Corral, V. Frette, J. Feder, and T. Jøssang, *Phys. Rev. Lett.* **77**, 107 (1996).
- [52] M. J. Aschwanden and S. L. Freeland, *Astrophys. J.* **754**, 112 (2012).
- [53] S. Manna, *Phys. A (Amsterdam)* **179**, 249 (1991).
- [54] P. Charbonneau, S. W. McIntosh, and T. J. Bogdan, *Sol. Phys.* **203**, 321 (2013).